

AccuLandNet: Enhancing Land Cover Detection with Deep Integrated Learning

Geetha Guthikonda¹, Dr. M. Senthil Kumaran²

Research Scholar, Dept. of CSE, SCSVMV University, Enathur, Kanchipuram, India¹

Asst. Professor, Dept. of IT, VR Siddhartha Engineering College, Kanuru, India¹

Associate Professor, Dept. of CSE, SCSVMV University, Enathur, Kanchipuram, India²

Abstract—Now-a-days, population growth is increasing more and more in all the places of the world. Specifically, this increase is in urban development based on economic and industrial improvement. It shows the massive impact on Land Use/Land Cover (LULC) and may change many times. The most popular use of land cover categorization is to analyze satellite imagery to categorize different land surface types, such as urban areas, agricultural fields, forests, and aquatic bodies. With the help of several land cover images, a unique classification model (UCM) based on satellite image classification will be developed in this study. The proposed approach implements the following stages. In the first stage, the pre-trained model U-Net was used to train the satellite images. In the second stage, the preprocessing techniques, including data acquisition and noise reduction, such as Adaptive Noise Removal (ANR) and Histogram Equalization (AHE), were used to preprocess the images. The third stage focused on extracting the features using Multi-Sensor Data Fusion (MSDF) to extract features like water bodies, roads, urban areas, edges, boundaries, and shapes. The final step uses the Maximum Likelihood Classification (MLC) combined with Support Vector Machines (SVM) to give the advanced classification results. Experimental results explain that the proposed approach outperformed the existing models in terms of better outcomes.

Keywords—Land Use/Land Cover (LULC); U-Net; Multi-Sensor Data Fusion (MSDF); Maximum Likelihood Classification (MLC); Support Vector Machines (SVM)

I. INTRODUCTION

Satellite images most commonly show the present Earth's region, which helps to improve the classification of Land Use and Land Cover (LULC) [1]. LULC mainly analyzes locations, urban development, ecological science, and natural resource management. Several components build the Earth's surface, which help in determining which activities belong to different land types [2]. Land cover mainly refers to the physical factors of the Earth's surface, including water features, urban infrastructure, and desert areas. The components implemented in this paper are metropolitan areas, grassy fields, swamps, and forest regions. The term "Land use" represents agriculture, urbanization, relaxation, and restoration [3]. This context mainly converts land usage for financial and societal purposes [4]. Land usage involves how humans use land, whereas land cover focuses primarily on the actual state of the land surface [5]. For example, forests (land cover) may be exploited for the manufacture of wood, preservation, or relaxation. Industrial zones and private sector commercials exist in an urban area (land cover, land uses).

Satellite images are essential in various applications, from disaster mitigation and crop evaluation to urban development and ecological surveillance. These images provide enormous data, both a chance and a difficulty [6]. Although the data includes fine-grained information about the Earth's surface, the vast amount of the data demands precise and efficient techniques for evaluation. Algorithms for machine learning (ML) have shown to be highly effective in deriving valuable data from satellite imagery. It has made it possible to classify land cover automatically, identify features, and track changes over time. ML provides a variety of techniques, each with advantages and disadvantages that can be used for classifying satellite images [7]. Cloud computing is one of the domains that help develop rapid applications using remote sensing technologies for monitoring crop classification. Google Earth Engine (GEE) is the cloud platform that analyzes environmental conditions and planetary analysis [8]. In this paper, the preprocessing is a critical step in LULC classification using remote sensing data. Effective preprocessing ensures the data is clean, consistent, and ready for analysis, leading to more accurate and reliable classification results. The pre-trained model trains the significant patterns belonging to LULC classification from the Landsat OLI (Vijayawada) dataset. For land cover classification using satellite images, integrating MLC and SVM takes advantage of both methods to increase classification consistency and efficiency.

Firstly, the Satellite Image Data Acquisition with raw satellite images is collected. Adaptive Noise Removal (ANR) is applied to these images to remove noise, while AHE (Histogram Equalization) is applied to improve the image's contrast/quality. The preprocessed images use Multi-Sensor Data Fusion (MSDF) to merge various sensor data to improve the accuracy of feature extraction. A Unique Classification Model (UCM) of MLC- SVM is applied to the features derived from the fused data. MLC makes a statistical assignment of each pixel to the most likely class, followed by SVM, which enhances the classification. Simultaneously, a pre-trained U-Net model, for instance, training, is used, and its knowledge is transferred to the classification pipeline with Transfer Learning to enhance performance. The last stage of the Result Analysis assesses an integrated model's classification accuracy and efficiency. This hybrid approach boosts precision and thus can be applied to land cover classification, vegetation mapping, and environmental monitoring.

The organization paper is designed as follows: Section I explains the introduction of LULC and its usage in various fields. Section II describes the literature survey by explaining multiple existing models and their performances. We have also identified research gaps that belong to various existing models. Section III describes the pre-trained model U-NET Architecture and its layers used to train on the LULC dataset. Section IV introduced the proposed methodology, which contains various techniques. Firstly, the preprocessing methods such as adaptive filtering (ANR) and AHE (Histogram Equalization), the feature extraction technique Multisensory data fusion (MSDF) are explained, and another model is Maximum Likelihood Classification (MLC). Finally, the MLC combined with SVM classified the LULC accurately and shows the results and discussions in Section V. Finally, the conclusion and future work are explained in Section VI.

II. LITERATURE SURVEY

Ansith et al. [9] gave an updated GAN architecture to enhance the resilience and accuracy of land use classification. The proposed system improves the classifier's capacity to discern between various land use categories by fusing a CNN for feature extraction with a GAN framework to produce realistic land use patterns. The updated GAN performs better than traditional CNN-based techniques, as evidenced by experimental results showing improved accuracy and better generalization across various datasets. The classification accuracy is improved by comparing it with various existing CNN algorithms. The accuracy of the suggested model was 96.2% on the UC Merced dataset, while a normal CNN only managed 92.5%. A CNN-based method for periodic multi-temporal pixel-based agricultural landscape classification was presented by Laban et al. [10]. The main goal is to increase classification accuracy by utilizing temporal sequences of satellite photos that capture the various crop species' phenological stages and seasonal fluctuations in land cover. Using a CNN architecture built to process sequential imagery and extract spatiotemporal features essential for differentiating between crop types and land cover classes, the suggested solution incorporates multi-temporal data from Sentinel-2 satellites. The results show that the CNN-based model outperforms previous methods with significantly higher accuracy (92.5%), F1-Score (0.91), and kappa coefficient (0.89), indicating its potential for operational usage in land management and agricultural surveillance. Thepade et al. [11] examined the differences between a number of Deep CNN models already in use to assess how well they categorize land use [26] from high-resolution aerial imagery. The suggested EfficientNet is appropriate for applications with constrained computational resources because it is optimized for both computational economy and performance. It is the recommended model for scenarios with computing limitations since it is optimal for obtaining the best accuracy with economical resource utilization. Our results show that accuracy (90.1%), precision (89.6%), recall (89.0%), and computational cost are generally better with deeper designs. This work offers insights into balancing resource limits and performance when choosing suitable models for certain applications.

Rao et al. [12] introduce a model that classifies satellite images of various land cover classes. The proposed model

collects the images and applies the DeepLabv3 (Atrous convolution) technique, which outperforms all other algorithms in categorizing land cover. It combines it with multiple atrous rates to acquire multi-scale data. The proposed system's performance reveals a high accuracy of 92.3% and an F1-score of 0.91 compared to current models. Varma et al. [13] proposed the FCNN algorithm with LandTrendr that detects changes in multi-spectral satellite images. The proposed approach uses the existing noise filters to remove the noise and spectral instability. Segmentation also plays a significant role in segmenting the images and analyzing the meaningful objects to find dynamic changes over time. The proposed approach's effectiveness was measured using several metrics, such as an accuracy of 89.78% based on NDVI, NBI, etc.

Fan et al. [14] proposed a novel feature learning approach (NFLA) recognizing the land-use scene with high-resolution images. The NFLA mainly uses the multiway sparse coding system to find multiple aspects in tedious sceneries. The proposed approach uses the BoW to extract various low-level features that consider the RGB and NIR data using patches with different sizes and several layers. The proposed NFLA was applied on three datasets with an accuracy of 87.67%, 88.45%, and 89.12%, respectively. Xia et al. [15] presented the DL-based model that automatically classifies the aerial scene classification from UC-Merced and WHU-RS19 datasets that show low performance, which is already implemented with limitations. The proposed approach uses the Aerial Image data set (AID), which is very large, with 10k aerial scene images. Finally, the proposed approach obtains the classification of 89.89% accuracy. Liu et al. [16] proposed MSCNN architecture for scene classification. Our MSCNN model leverages multiple input image scales to learn global and local features effectively. By integrating different scales, the network can comprehend the intricate patterns and textures across various scenes. The experimental results indicate that MSCNN achieved an accuracy of 83.5%, outperforming the previous best model, which had an accuracy of 79.6% for the MIT Indoor 67 dataset. For the SUN397 dataset, the MSCNN recorded an accuracy of 76.3%, compared to 73.4% by the previous leading method. For the Places365 dataset, MSCNN obtained an accuracy of 88.1%, surpassing the previous best of 85.7%.

Ouerghi et al. [17] proposed an automated model that detects changes between pairs of satellite images taken at different times. Our approach leverages CNN architecture, specifically a U-Net, due to its proven effectiveness in image segmentation tasks. We trained our model on a publicly available dataset containing annotated satellite images depicting various changes. The results achieved a Precision of 0.88, a recall score of 0.85, an F1 score of 0.86, and an IoU of 0.78. Peng et al. [18] proposed that the novel end-to-end Change detection (CD) method contains an encoder-decoder system with advanced segmentation called UNet++. This model connects the image pairs with local and fine-tuned data that generates the feature maps. The performance is improved by adopting the fusion approach with UNet++, which works on multiple sides and combines maps at various levels. Results show that the proposed approach shows effective outcomes with a high accuracy of 92.12%. Chen et al. [19] introduced the

model that finds the changes detected in images. The main aim of this approach is to change the data and remove the irrelevant noise, improving the proposed algorithm's performance. The existing approaches overcome the lack of accuracy, which leads to low performance. The dual attention fully convolutional Siamese networks mainly focused on detecting the changes obtained in high-quality images. Experiments show that the proposed approach obtains 3.1% to 4.3% of F1-score improvements. Cai et al. [20] introduced the DenseNets model, which addresses several problems. The proposed approach finds accurate remote-sensing images by using the new landslip sample collection. The suggested landslip detection method identifies the three distinct Gorges reservoir sites in China. The suggested DenseNets' performance enhanced the F1 score and kappa of 0.9505 and 0.9474.

III. PRE-TRAINED MODEL: U-NET ARCHITECTURE

The U-NET architecture belongs to the CNN model that can be used in several image segmentation applications. In this scenario, the U-NET mainly focused on LULC analysis. It is well-suited for land cover classification using images from satellites because of its capacity to deliver accurate localization and context in image data [28]. Fig. 1 shows the architecture of pre-trained model.

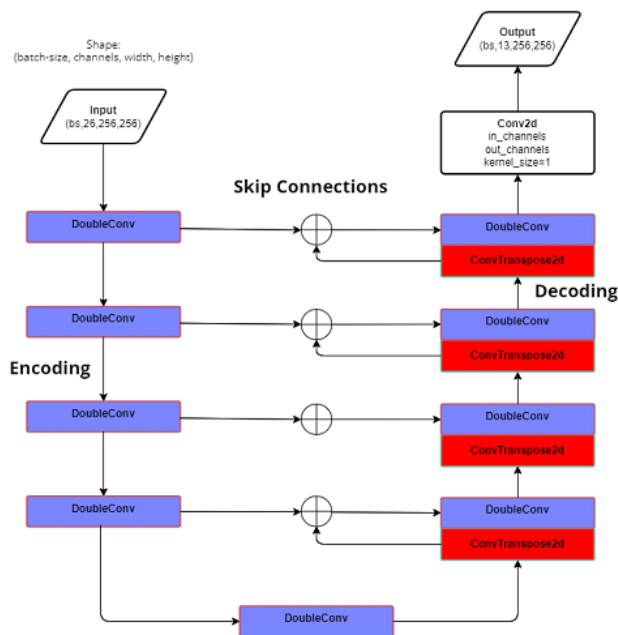


Fig. 1. U-NET architecture for training the land cover images.

1) *Encoder*: In U-NET, the encoder uses a series of convolutional layers and max-pooling techniques to extract the context from the input image. This route is in charge of extracting hierarchical features by minimizing the spatial dimensions and improving the level of feature maps.

$$\text{Convolution: } K = M * A + y \quad (1)$$

$$\text{ReLU Activation: } A = \text{ReLU}(Z) \quad (2)$$

$$\text{Max Pooling: } B = \text{Maxpool}(C) \quad (3)$$

Where * stands for the convolution process, ReLU for the rectified linear unit function, and M and y for the convolutional layer's weights and bias.

2) *Bottleneck*: The network has a bottleneck when the feature mappings are the most abstract and the spatial resolution is the lowest near the bottom of the U-shape.

3) *Decoder*: Up-sampling methods and convolutional layers are used in the decoder route to reconstruct the spatial dimensions sequentially. This method preserves geographic data dropped throughout the down-sampling method by using skip connections originating from the encoder's respective layers. The final output will retain fine-grained details thanks to these skip connections. In up-sampling layer, two convolutional layers, and ReLU activations follow each step in the expanding path. These are followed by a concatenation with the equivalent feature map from the contracting path.

$$Y = \text{Concat}(U, A_{\text{encoder}}) \quad (4)$$

4) *Output layer*: A 1x1 convolutional layer, the last layer in the U-NET, maps every feature vector with 64 components to the number of classes required for land cover segment.

$$\text{Final Convolution: } K = M * A + y \quad (5)$$

$$\hat{Y} = \text{Softmax}(Z) \quad (6)$$

Using satellite imagery, the U-NET architecture has shown to be an effective method for classifying land cover. It is especially well-suited for this application because of its capacity to integrate spatial and contextual data. Accurate and scalable land cover classification will become more and more possible as machine learning techniques and satellite imagery data become more widely available. This will have a major impact on a number of fields, including disaster management, agriculture, urban planning, and environmental monitoring.

IV. PROPOSED METHODOLOGY

In this section, the proposed methodology is discussed in various steps. Fig. 2 describes the pipeline for satellite image classification with proposed approach.

A. Pre-Processing Techniques

Preprocessing the satellite images contains multiple systematic steps to prepare (or make ready) the pictures for further analysis. These methods are mainly used for feature normalization by removing the noise and highlighting the dark regions that help to classify the accurate land covers. The first step uses noise removal with adaptive filtering (ANR) and AHE (Histogram Equalization), which removes noise and enhances the contrast of the image. When using these two concepts, the Land cover classification results of the satellite images may be undistorted/unbiased from errors and thus more visually comparable. This section further explains the mathematical equations of these methods used in the capturing of satellite images and highlights their main purpose in land cover [27] type in the entire flow of the land cover classification system. Table I shows the comparative performance of algorithms.

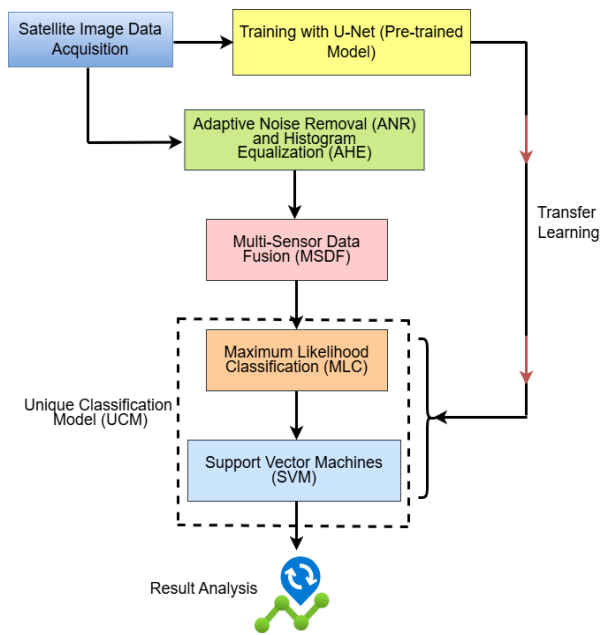


Fig. 2. System architecture.

TABLE I. COMPARATIVE PERFORMANCE OF ALGORITHMS

Authors	Proposed Approach	Performance Metrics	Research Gaps
Li et al. [21]	Multisource CD UNet++	MSOSCD the IoU-87.05% and F1-Score-93.1% and for MSBC dataset the IoU-87.05% and F1-Score-65.77%.	Lack of stable outcomes in terms of accurate locations with multisource features.
Thepade et al. [22]	DCNN	Accuracy (%) of 97.94, Precision (%) of 97.96, Recall (%) of 97.94, and F1-Score (%) of 97.94.	Lack of color based extraction is required to improve the performance.
Jagannathan et al. [23]	Hybrid Hot Encoding VGG19	Accuracy of 98.5%	The training with ResNet50 is very unclear.
Bin Xia et al. [24]	CNN	Accuracy of 0.9472, Misclassification rate of 0.0528, and kappa coefficient of 0.9435.	There is a lack of factors semantic data, obstruction, and distortion
Sudeep et al. [25]	Thepade SBTC	Acc of 70%, MCC of 0.68, and F1-score of 0.69.	Lack of feature extraction in terms of land usage finding from aerial images.

B. Multi-Sensor Data Fusion (MSDF)

Feature extraction plays a crucial role in LCLU. The main functionality of feature extraction is to convert the raw data into a list of features that can be used to conduct further analysis. Multisensory data fusion (MSDF) takes one step further in improving the accuracy and reliability of the derived characteristics by aggregating information from multiple sensors. The MSDF integrates information from various sensors more robustly and precisely. These sensors improve data quality and filter noise, which affects system performance. It also condenses the raw, unprocessed sensor data to simpler, more meaningful features. Next, autonomous navigation, environmental observation, object discovery, etc., can use these

features with more relevant and discriminative inputs with the effect of feature extraction that can significantly enhance the algorithms in these applications.

The following formulations are most widely used to measure the features:

Weighted Averaging: It is very easy to measure the weighted average of the sensor measurements thus, the weight is derived based on the accuracy of each sensor.

$$W = \sum_{i=1}^n w_i a_i \quad (7)$$

Kalman Filter: It is used for the sensor fusion specifically applications like LCLU.

$$\hat{a}_k = \hat{a}_{k-1} + K_k(c_k - H\hat{a}_{k-1}) \quad (8)$$

C. Maximum Likelihood Classification (MLC)

The MLC is the classification method that covers the land applied in GIS (geographic information systems) and remote sensing. Transfer learning trains the samples by utilizing the statistical factors of pixel values to specify the land cover. The probability of every pixel measures the members of each class by using the probability density function of multidimensional normal distribution—the pixel of every class placed with high potential possibility. The MLC is very effective and easy to classify into different effectively distributed and separated classes. Suppose the class distributions overlap, and then the performance drops low. Finally, the likelihood that every pixel in the image belongs to every land cover class by using the Gaussian (normal) distribution model. In this context, the highest probability (maximum likelihood) pixels are represented with the specific class.

The probability $P(A|Z_i)$ that a pixel feature vector A belongs to class Z_i is given by the multivariate normal distribution.

$$P(A|Z_i) = \frac{1}{(2\pi)^{d/2} |\Sigma_i|^{1/2}} \exp\left(-\frac{1}{2}(A - \mu_i)^T \Sigma_i^{-1}(A - \mu_i)\right) \quad (9)$$

D. Support Vector Machines (SVM)

SVMs perform remarkably well in binary classification applications. SVM can easily handle high-dimensional feature spaces, which is common in remote sensing data. It finds the feature space hyperplane that most effectively separates the classes. SVM maximizes the margin between data points of distinct classes, which lowers the risk of overfitting, particularly in higher-dimension domains. The kernel approach maps input space to a high dimensional space and allows SVM to classify non-linearly. SVM maps the input data to a higher dimensional space where a linear separation is possible using kernel functions when the data are not linearly separable. The standard base kernels are the polynomial, sigmoid, and radial basis functions (RBF). The margin is between the hyperplane and the nearest points of both classes. This margin must be maximized via SVM. Since these data are the most trustworthy and closest to the selection border (hyperplane), they are essential for determining the precise location and orientation of the hyperplane.

The binary classification issue is solved by using training dataset $\{(a_i, b_i)\}_{i=1}^N$, Where $x_i \in R^n$ represents feature vector

and $y_i \in \{-1, 1\}$ class label helps to find the maximum margin.

The equation of a hyperplane in an n-dimensional space is:

$$w \cdot x - b = 0 \quad (10)$$

Here, w is the normal vector to the hyperplane, and b is the bias term.

To ensure correct classification, the following constraints must be satisfied:

E. Optimization Problem

The objective is to maximize the margin, which is equivalent to minimizing $\|w\|$, subject to the constraints above. The optimization problem can be formulated as:

$$\min_{w,b} \frac{1}{2} \|w\|^2 \quad (11)$$

Subject to $y_i(w \cdot x_i - b) \geq 1, i = 1, \dots, N$

Lagrangian Formulation

Using Lagrange multipliers α_i , the issue can be represented as:

$$\mathcal{L}(w, b, \alpha) = \frac{1}{2} \|w\|^2 - \sum_{i=1}^N \alpha_i [y_i(w \cdot x_i - b) - 1] \quad (12)$$

By solving this dual problem, we get:

$$\max_{\alpha} \sum_{i=1}^N \alpha_i - \frac{1}{2} \sum_{i=1}^N \sum_{j=1}^N \alpha_i \alpha_j y_i y_j (x_i \cdot x_j) \quad (13)$$

Subject to $\sum_{i=1}^N \alpha_i y_i = 1, \alpha_i \geq 0$.

The optimal w is given by:

$$w = \sum_{i=1}^N \alpha_i y_i x_i \quad (14)$$

Finally, the SVM model can classify new, unseen data points (pixels) into land cover classes based on the learned decision function:

$$f(x) = \text{sign}(w \cdot x - b) \quad (15)$$

F. Combination of MLC and SVM

The combination of SVM and other methods obtains a high classification rate based on land cover. The MLC is a reliable method that works effectively on various types of satellite images and land cover situations, helping to increase the accuracy of classification.

G. Dataset Description

The dataset mainly gather the information of Vijayawada as of 24-10-2022 as shown in Fig. 3 and Fig. 4. Vijayawada is situated on the banks of the Krishna River, in the geographic middle of the Andhra Pradesh state in India, it is a historic city with coordinates of 16°03'11" N and 80°03'91" E. Equatorial weather prevails, with warm summers and mild winters. In May and June, the temperature peaks at 47 °C, whereas in the winter, it ranges from 20 to 27 °C. The average annual rainfall is 103 cm, while the average humidity is 78%.

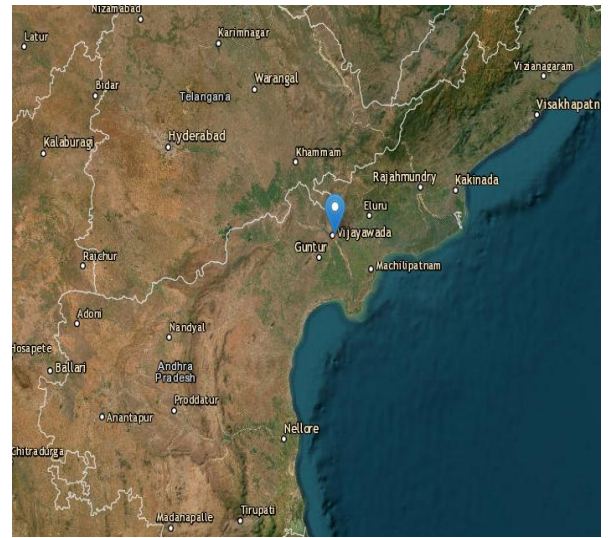


Fig. 3. Sample Vijayawada city map collected from USGS database.

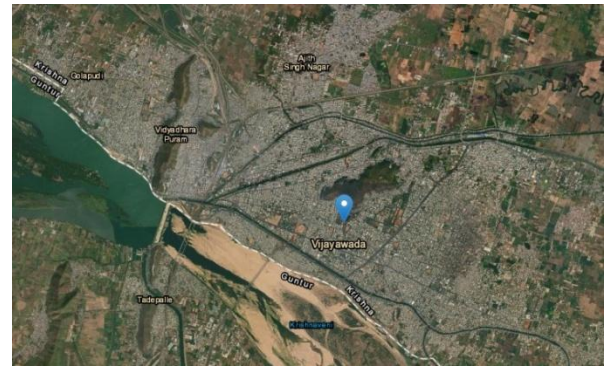


Fig. 4. This is the actual MAP of Vijayawada as on 24-10-2022.

V. RESULTS AND DISCUSSIONS

A. Performance Metrics

The following parameters show the performance of ML algorithms applied on USGS dataset. The classified image contains five classes' building_regions, green_lands, farmlands, sandlands and water_regions. All these regions are marked with various colors. The confusion matrix is calculated and obtained results are compared with existing system results.

$$\text{Accuracy (ACC)} = \frac{TP + TN}{TP + TN + FP + FN}$$

$$\text{Precision (Pre)} = \frac{TP}{TP + FP}$$

$$\text{Specificity (Sp)} = \frac{TN}{TN + FP}$$

$$\text{Recall (Re)} = \frac{TP}{TP + FN}$$

$$F1 - \text{Score (F1S)} = 2 * \frac{(\text{Precision} * \text{Recall})}{(\text{Precision} + \text{Recall})}$$

B. Discussions

The algorithms were implemented using the Python programming language. Each algorithm obtained the count values based on the actual values and predicted values. The existing models, such as the Change detection network (CDNet) and fully convolutional-early fusion (FC-EF), were compared with the proposed approach.

Table II describes the classification performance of existing CDNet model based on the count values belongs to five classes shown in Fig. 5. The average (acc) of all the classes is 0.72%, pre of 0.72%, (re) of 0.71%, (spc) of 0.92%, and F1S of 0.72%. Among all the parameters the specificity shows the high values that represents the imbalance in binary classification.

TABLE II. PERFORMANCE OF CDNET BASED ACTUAL VALUES AND PREDICTED VALUES

LCLU	Acc	Pre	Re	Spc	F1S
Building Regions	0.72	0.66	0.72	0.91	0.69
Green Lands	0.72	0.74	0.69	0.93	0.71
Farm Lands	0.72	0.71	0.69	0.93	0.70
Sand Lands	0.72	0.74	0.78	0.93	0.76
Water Regions	0.72	0.74	0.71	0.93	0.73

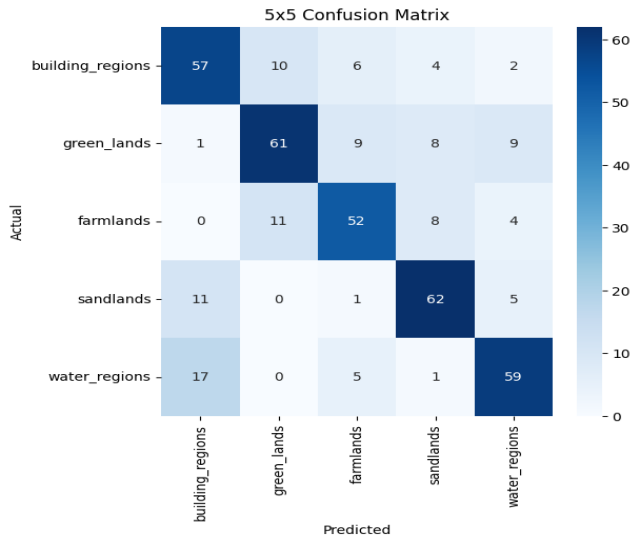


Fig. 5. Count values obtained from 5x5 confusion matrix using CDNet.

TABLE III. PERFORMANCE OF FC-EF BASED ACTUAL VALUES AND PREDICTED VALUES

LCLU	Acc	Pre	Re	Spc	F1S
Building Regions	0.80	0.81	0.75	0.95	0.77
Green Lands	0.80	0.81	0.76	0.95	0.78
Farm Lands	0.80	0.76	0.75	0.94	0.75
Sand Lands	0.80	0.75	0.89	0.93	0.81
Water Regions	0.80	0.84	0.83	0.96	0.83

Table III describes the classification performance of existing FC-EF model based on the count values belongs to five classes shown in Fig. 6. The average (acc) of all the classes is 0.80%, (pre) of 0.83%, (re) of 0.796%, (spc) of 0.94%, and F1S of 0.79%. Among all the parameters the

specificity shows the high values that represents the imbalance in binary classification.

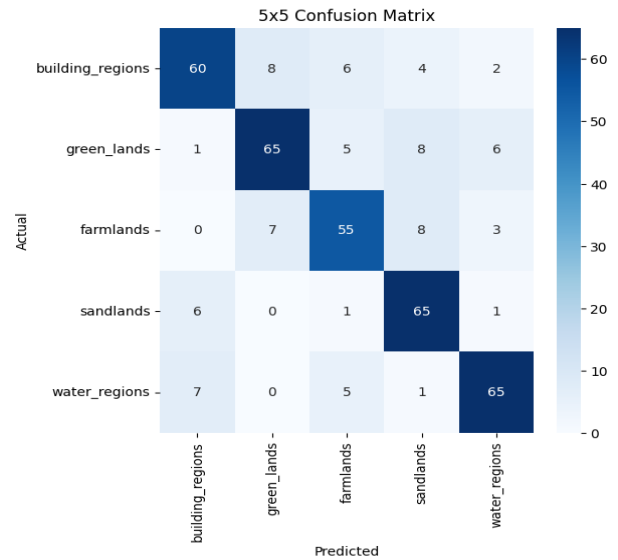


Fig. 6. Count values obtained from 5x5 confusion matrix using FC-EF.

TABLE IV. PERFORMANCE OF PROPOSED BASED ACTUAL VALUES AND PREDICTED VALUES

LCLU	Acc	Pre	Re	Spc	F1S
Building Regions	0.93	0.97	0.91	0.99	0.94
Green Lands	0.93	0.92	0.91	0.97	0.91
Farm Lands	0.93	0.87	0.91	0.97	0.89
Sand Lands	0.93	0.91	0.97	0.97	0.94
Water Regions	0.93	0.98	0.94	0.99	0.96

Table IV describes the classification performance of existing FC-EF model based on the count values belongs to five classes shown in Fig. 7. The average (acc) of all the classes is 0.93%, (pre) of 0.95%, (Re) of 0.95%, (spc) of 0.98%, and F1S of 0.97%. Compare with above algorithms the proposed approach shows the high performance.

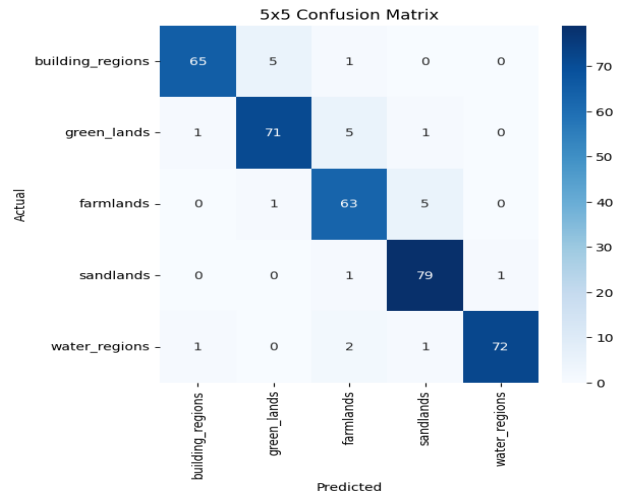


Fig. 7. Count values obtained from 5x5 confusion matrix using proposed approach.

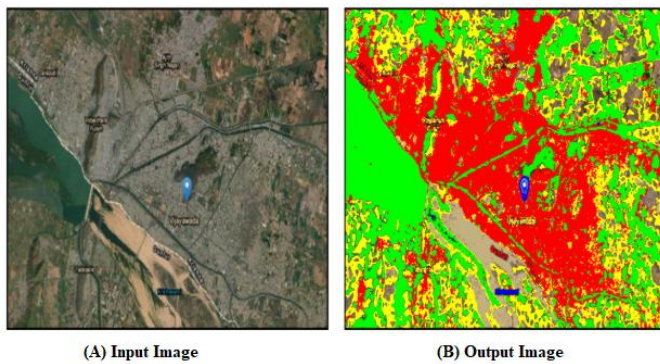


Fig. 8. (A) Input image, (B) Output image after implementation with the proposed MLC and SVM.

VI. CONCLUSION

The proposed MLC combines U-NET as a pre-trained model that transfers the LULC patterns to the proposed SVM algorithm. Other preprocessing techniques, such as ANR and AHE ref, refine image noise, extract significant features using MSDF, and handle high-dimensional data and non-linear relationships. The proposed approach is also a Unique Classification Model (UCM) that classifies the accurate LULC regions in the datasets. The Integrated SVM effectively improves classification in this work by focusing on the critical support vectors that define the class separations. Despite the increased computational complexity of integrating MLC and SVM, the algorithm remains scalable and efficient. Finally, the proposed approach obtains high performance in terms of average accuracy of all the classes of 0.93%, precision of 0.95%, recall of 0.95%, specificity of 0.98%, and 0.97% based on five classes such as building_regions, green_lands, farmlands, Sandilands, and water_regions as shown in Fig. 8 and Table V. Compared with the above algorithms, the proposed approach shows a high performance. In the future, high-quality images will require finding the various land types using ecosystem mapping and satellite imagery with accurate region classification. Also, developed the integrated models to detect and classify various deep learning models combined with image processing to show high impact on LULC regions.

TABLE V. THE DIFFERENT LAND TYPES COVERED WITH VARIOUS COLORS

Colors	Regions
Red	Buildings
Green	Greenery Lands
Yellow	Agricultural Lands
Sandy Brown	Sand Lands
Blue	Water regions

REFERENCES

- [1] H. Ouchra and A. Belangour, "Satellite image classification methods and techniques: A survey," in Proc. IEEE Int. Conf. Imag. Syst. Techn. (IST), Aug. 2021, pp. 1–6, doi: 10.1109/IST50367.2021.9651454.
- [2] S. Jalayer, A. Sharifi, D. Abbasi-Moghadam, A. Tariq, and S. Qin, "Modeling and predicting land use land cover spatiotemporal changes: A case study in Chalus watershed, Iran," IEEE J. Sel. Topics Appl. Earth Observ. Remote Sens., vol. 15, pp. 5496–5513, 2022, doi: 10.1109/JSTARS.2022.3189528.
- [3] A. Tassi and M. Vizzari, "Object-oriented LULC classification in Google Earth Engine combining SNIC, GLCM, and machine learning algorithms," Remote Sens., vol. 12, no. 22, pp. 1–17, Nov. 2020, doi: 10.3390/rs12223776.
- [4] M. A. Shafaey, M. A. M. Salem, H. M. Ebied, M. N. Al-Berry, and M. F. Tolba, "Deep learning for satellite image classification," in Proceedings of the International Conference on Advanced Intelligent Systems and Informatics 2018 (Advances in Intelligent Systems and Computing). Springer-Verlag, 2019, pp. 383–391, doi: 10.1007/978-3-319-99010-1_35.
- [5] M. Esmaili, D. Abbasi-Moghadam, A. Sharifi, A. Tariq, and Q. Li, "Hyperspectral image band selection based on CNN embedded GA (CNNeGA)," IEEE J. Sel. Topics Appl. Earth Observ. Remote Sens., vol. 16, pp. 1927–1950, 2023, doi: 10.1109/JSTARS.2023.3242310.
- [6] S. Mahyoub, H. Rhinane, A. Fadil, M. Mansour, M. Saleh, and F. Al-Nahmi, "Using of open access remote sensing data in Google Earth Engine platform for mapping built-up area in Marrakech city, Morocco," in Proc. IEEE Int. Conf. Moroccan Geomatics (Morgeo), May 2020, pp. 1–5, doi: 10.1109/MORGE049228.2020.9121912.
- [7] M. Amani, A. Ghorbanian, S. A. Ahmadi, M. Kakooei, A. Moghimi, S. M. Mirmazloumi, S. H. A. Moghaddam, S. Mahdavi, M. Ghahremanloo, S. Parsian, Q. Wu, and B. Brisco, "Google Earth Engine cloud computing platform for remote sensing big data applications: A comprehensive review," IEEE J. Sel. Topics Appl. Earth Observ. Remote Sens., vol. 13, pp. 5326–5350, 2020, doi: 10.1109/JSTARS.2020.3021052.
- [8] M. Awad, "Google Earth Engine (GEE) cloud computing based crop classification using radar, optical images and support vector machine algorithm (SVM)," in Proc. IEEE 3rd Int. Multidisciplinary Conf. Eng. Technol. (IMCET), Dec. 2021, pp. 71–76, doi: 10.1109/IMCET53404.2021.9665519.
- [9] S. Ansith and A. A. Bini, "A modified Generative Adversarial Network (GAN) architecture for land use classification," 2021 IEEE Madras Section Conference (MASCON), Chennai, India, 2021, pp. 1-6, doi: 10.1109/MASCON51689.2021.9563609.
- [10] N. Laban, B. Abdellatif, H. M. Ebeid, H. A. Shedeed and M. F. Tolba, "Seasonal Multi-temporal Pixel Based Crop Types and Land Cover Classification for Satellite Images using Convolutional Neural Networks," 2018 13th International Conference on Computer Engineering and Systems (ICCES), Cairo, Egypt, 2018, pp. 21–26, doi: 10.1109/ICCES.2018.8639232.
- [11] S. D. Thepade, S. S. Adrakatti, S. Chauhan, V. Chitnis and A. Bhalerao, "Comparing the Deep Convolutional Neural Network Models for Identification of Aerial Image Land Use," 2023 7th International Conference On Computing, Communication, Control And Automation (ICCUBEA), Pune, India, 2023, pp. 1-7, doi: 10.1109/ICCUBEA58933.2023.10392161.
- [12] D. R. Rao, S. Noorjahan and S. A. Fathima, "Classification of Land Cover Usage from Satellite Images using Deep Learning Algorithms," 2022 International Conference on Electronics and Renewable Systems (ICEARS), Tuticorin, India, 2022, pp. 1302-1308, doi: 10.1109/ICEARS53579.2022.9752282.
- [13] N. A. K. Varma, S. Manne and P. L. Sri, "Object based Change detection on Temporal Multi-Spectral Satellite imagery," 2023 6th International Conference on Recent Trends in Advance Computing (ICRTAC), Chennai, India, 2023, pp. 354-359, doi: 10.1109/ICRTAC59277.2023.10480725.
- [14] J. Fan, T. Chen and S. Lu, "Unsupervised Feature Learning for Land-Use Scene Recognition," IEEE Transactions on Geoscience and Remote Sensing, vol. 55, no. 4, pp. 2250-2261, April 2017.
- [15] G.-S. Xia, J. Hu, F. Hu, B. Shi, X. Bai, Y. Zhong, et al., "AID: A benchmark data set for performance evaluation of aerial scene classification," IEEE Trans. Geosci. Remote Sens., vol. 55, no. 7, pp. 3965-3981, Jul. 2017.
- [16] Y. Liu, Y. Zhong and Q. Qin, "Scene classification based on multiscale convolutional neural network," IEEE Trans. Geosci. Remote Sens., vol. 56, no. 12, pp. 7109-7121, Dec. 2018.

- [17] E. Ouerghi, "A Deep Learning Model for Change Detection on Satellite Images", *Image Processing On Line*, Nov. 2022.
- [18] D. Peng, Y. Zhang and H. Guan, "End-to-End Change Detection for High Resolution Satellite Images Using Improved UNet++", *Remote Sensing*, Jun. 2019.
- [19] J. Chen et al., "DASNet: Dual Attentive Fully Convolutional Siamese Networks for Change Detection in High-Resolution Satellite Images", *IEEE Journal of Selected Topics in Applied Earth Observations and Remote Sensing*, Jan. 2021.
- [20] H. Cai, T. Chen, R. Niu and A. Plaza, "Landslide Detection Using Densely Connected Convolutional Networks and Environmental Conditions", *IEEE Journal of Selected Topics in Applied Earth Observations and Remote Sensing*, May 2021.
- [21] H. Li, F. Zhu, X. Zheng, M. Liu and G. Chen, "MSCDUNet: A Deep Learning Framework for Built-Up Area Change Detection Integrating Multispectral SAR and VHR Data", *IEEE Journal of Selected Topics in Applied Earth Observations and Remote Sensing*, Jan. 2022.
- [22] S. D. Thepade and M. R. Dindorkar, "Fusing deep convolutional neural network features with Thepade's SBTC for land usage identification", *Engineering Science and Technology an International Journal*, vol. 27, pp. 101014, Mar. 2022.
- [23] J Jagannathan and C Divya, "Deep learning for the prediction and classification of land use and land cover changes using deep convolutional neural network", *Engineering Science and Technology an International Journal*, vol. 65, pp. 101412, Aug 2021.
- [24] Bin Xia, Fanyu Kong, Jun Zhou, Xin Wu and Qiong Xie, "Land Resource Use Classification Using Deep Learning in Ecological Remote Sensing Images", *Hindawi Computational Intelligence and Neuroscience*, vol. 2022, pp. 7179477.
- [25] D Sudeep, Thepade and Piyush R. Chaudhari, "Land Usage Identification with Fusion of Thepade SBTC and Sauvola Thresholding Features of Aerial Images Using Ensemble of Machine Learning Algorithms", *Applied Artificial Intelligence*, vol. 35, no. 2, pp. 154-170, Nov 2020.
- [26] Q. Weng, Z. Mao, J. Lin and W. Guo, "Land-use classification via extreme learning classifier based on deep convolutional features", *IEEE Geosci. Rem. Sens. Lett.*, vol. 14, no. 5, pp. 704-708, 2017.
- [27] R. Stivaktakis, G. Tsagkatakis and P. Tsakalides, "Deep learning for multilabel land cover scene categorization using data augmentation", *IEEE Geosci. Rem. Sens. Lett.*, vol. 16, no. 7, pp. 1031-1035, 2019.
- [28] A. Clark, S. Phinn, and P. Scarth, "Optimised U-Net for land use-land cover classification using aerial photography", *PFG – J. Photogramm. Remote Sens. Geoinf. Sci.*, vol. 91, no. 2, pp. 125–147, Apr. 2023.